Design and 3D printing of lower limb prosthetic socket with metamaterials for performance enhancement

OPEN ACCESS
IOP Publishing
Smart Materials and Structures
Smart Mater. Struct. **34** (2025) 125035 (12pp)
https://doi.org/10.1088/1361-665X/ae2812

Design and 3D printing of lower limb prosthetic socket with metamaterials for performance enhancement

Sheng Li[1], Mahdi Bodaghi[2], Guoxin Fang[3], Wenbin Qiu[4], Xinyu Wu[1] and Fei Gao[1,*]

[1] Shenzhen Institute of Advanced Technology, Chinese Academy of Sciences, Shenzhen 518055, People's Republic of China
[2] Department of Engineering, School of Science and Technology, Nottingham Trent University, Nottingham NG11 8NS, United Kingdom
[3] Department of Mechanical and Automation Engineering, The Chinese University of Hong Kong, Hong Kong Special Administrative Region of China, People's Republic of China
[4] Department of Fundamental Courses, Wuxi University of Technology, Wuxi 214121, People's Republic of China

E-mail: gaofeicsu104@gmail.com

Received 22 July 2025, revised 14 October 2025
Accepted for publication 4 December 2025
Published 15 December 2025

Abstract

Globally, there are over 15 million individuals with lower limb amputations. Traditional prosthetic sockets, limited by handcrafting technology, frequently lack an optimal fit with the residual limb, leading to residual limb pain, skin abrasion, and compensatory gait. This paper presents an innovative version of prosthetic socket to optimize pressure distribution on the residual limb and enhance amputee's comfort by introducing the zero Poisson's ratio metamaterials. First, the musculoskeletal model of the residual limb was constructed using computed tomography data and divided into pressure-tolerant and pressure-sensitive zones based on biomechanical principles. The zero Poisson's ratio metamaterials were embedded in the patellar tendon region to reduce localized stress concentration. The prosthetic socket, structurally optimized through finite element analysis, was fabricated using 3D printing technology and validated via flexible pressure sensing and gait experiments. Simulation results showed that the zero Poisson's ratio metamaterials reduced skin stress in the patellar tendon region from 97.84 kPa (biomechanically designed prosthetic socket) to 83.74 kPa, achieving a 14.4% reduction. Human experiments further demonstrated a 11.7% decrease in peak walking pressure (145 kPa to 128 kPa). Furthermore, the knee joint symmetry coefficient during

* Author to whom any correspondence should be addressed.

squatting improved from 0.992 to 0.999 when comparing the original socket to the zero Poisson's ratio metamaterials socket. This method provides an efficient and precise solution for personalized prosthetic socket design, with the potential to enhance the mobility of amputees.

Keywords: prosthetic socket, zero Poisson's ratio metamaterial, biomechanical optimization, FEA, 3D printing, human testing

1. Introduction

There are over 30 million amputations worldwide mostly caused by diabetes, traffic accidents, and armed conflict [1]. In addition, over half of them suffer from lower limb amputation. Prosthetic devices [2–4] play a crucial role in restoring mobility and improving the life quality of amputees. With the advance in manufacturing technology, old version of passive prostheses have been gradually replaced by powered prostheses which enable more natural and energetic gait. The active prosthetic system typically comprises components including the prosthetic foot, metal pylons, prosthetic socket, and liner, as shown in figure 1. Among them, the prosthetic socket [5, 6] is an essential unit for connecting the residual limb to the prosthesis, transmitting forces, providing suspension, facilitating control, and ensuring comfort. Therefore, a nicely designed prosthetic socket can guarantee the function of a prosthetic system and offer a cozy environment for amputees, as well.

To further improve amputees' experience with prosthetic system, various types of prosthetic sockets have been developed. For instance, adjustable prosthetic sockets [8, 9] can precisely meet the special needs of early-stage amputees, children, and individuals living in remote areas. However, such products require particular skills of prosthetists and are more prone to stress concentration after repeated adjustments. The problematic heat dissipation around residual limb can be addressed by hollowed-out designs to reduce the weight and heat accumulation of prosthetic sockets [10, 11], but the structural strength has to be compromised. Another approach combines fans with spiral air channels to enhance heat dissipation [12, 13] with the shortcoming of bulky and energy-consuming. Aiming at pressure-sensitive areas of the residual limb subjected to prosthetic sockets, 3D printing technology were employed to combine rigid and flexible materials for pressure alleviation in specific zones [14, 15]. Nevertheless, this manufacturing process is still challenging, and the long-term fatigue performance of the structure requires further validation. An alternative solution used air bladders to fill pressure-sensitive areas for pressure relief [16, 17], but the structural complexity downgraded its usability. In fact, the amputees' residual limb lacks the evolutionary adaptability of natural human anatomy and does not possess specialized pressure-tolerant regions like the plantar surface. Consequently, pressure concentrates on specific pressure-tolerant regions of the residual limb, primarily including the patellar tendon, popliteal fossa, lateral tibial, and medial tibial regions. Notably, the patellar tendon region withstands the highest pressure, which increases significantly under specific conditions (such as squatting and heel strike), severely exacerbates the amputees' experience.

For the sake of improving the comfort level of prosthetic socket wearers, we have proposed the utilization of metamaterial structures [18–22] to alleviate pressure concentration. In general, conventional structures (hexagonal honeycombs) with positive Poisson's ratio exhibit lateral expansion during transverse compression, which are obviously unsuitable for prosthetic socket applications. On the contrary, negative Poisson's ratio structures (concave hexagons, rotating rigid units, chiral structures) demonstrate unique advantages such as superior energy absorption [23–26], but their tendency for lateral contraction under compression limits application in pressure-tolerant zones of prosthetic sockets. Hence, the zero Poisson's ratio metamaterial, which show potential as energy absorbers in automotive, railway, and aerospace engineering [27, 28], is proposed as promising candidates for prosthetic socket applications with better performance. In detail, the zero Poisson's ratio metamaterial is featured by the absence of lateral strain under longitudinal strain during elastic compression. Our previous research [29, 30] has demonstrated the superior reversible energy absorption capabilities of zero Poisson's ratio metamaterials compared to the negative counterpart, demonstrating their great potential for prosthetic socket applications. Furthermore, the rapid development in 3D printing technology further provides robust technical support for fabricating such complex structures.

In this work, we propose a novel prosthetic socket with zero Poisson's ratio metamaterials to optimize pressure distribution. This methodology includes residual limb modeling, socket design, finite element analysis (FEA) optimization, and 3D printing. Specifically, an accurate musculoskeletal model of the residual limb is firstly established using computed tomography (CT) data, followed by the designing of prosthetic socket according to biomechanical principles, the introducing of the zero Poisson's ratio metamaterials into the pressure-tolerant zone (patellar tendon), the evaluation of stress distribution by FEA, and the fabrication of the prosthetic socket component via 3D printing technology. Finally, the pressure distribution of residual limb was characterized using the flexible pressure transducer, and preliminary squatting experiments were performed to verify the comfort of the prosthetic socket. This research aims to improve the current techniques for fabricating prosthetic sockets, potentially reducing the economic burden of prostheses for millions of disabled individuals and enhancing the interactive experience of wearing a prosthesis.

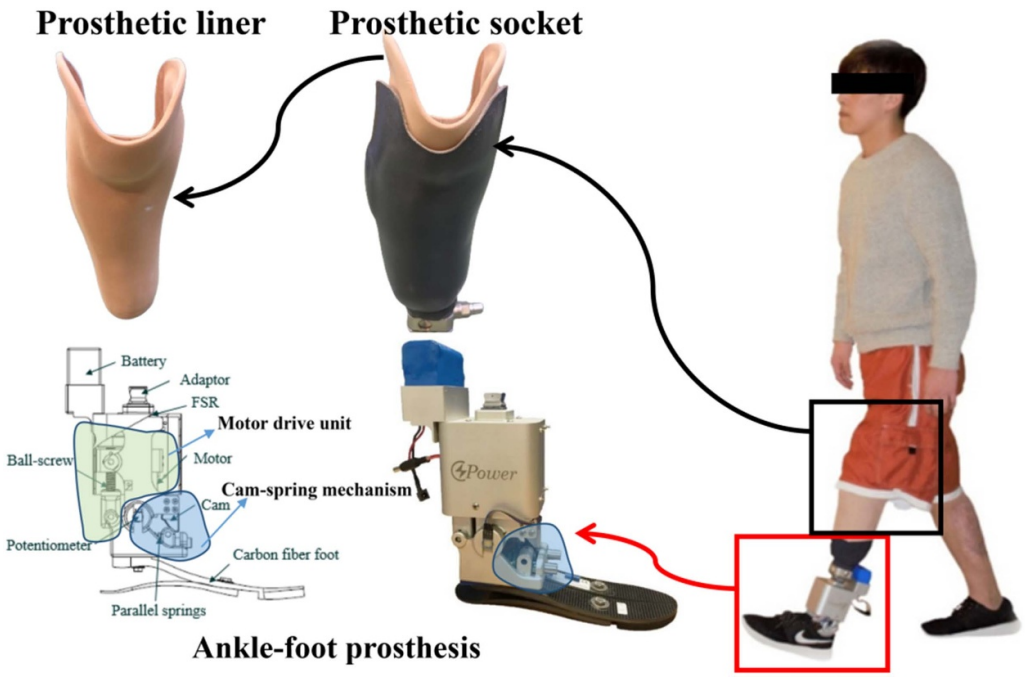

Figure 1. A powered ankle-foot prosthesis with a nonlinear parallel previously developed by the authors' team [7]. The integration includes the motor drive unit, cam-spring mechanism, carbon fiber foot, battery, and adaptor. The prosthetic socket is employed to attach the prosthesis to the residual limb. Republished with permission of ASME, from [7].

2. System design

This work focused on the model design, pressure distribution, and standing and squatting movements testing of the prosthetic socket with zero Poisson's ratio metamaterials, which was conducted at the Shenzhen Institute of Advanced Technology, Chinese Academy of Sciences, Shenzhen, China. The research was conducted in accordance with the principles embodied in the Declaration of Helsinki and in accordance with local statutory requirements. Ethical approval for this study was obtained (Document No. SIAT-IRB-240 315-H0713), and the subject gave written informed consent to participate in the study before any testing. A female amputee with tibial amputation was recruited for this study (40 years, 160 cm height, 52 kg weight, 15 years post-amputation).

2.1. Zero Poisson's ratio metamaterials characterization

In this work, we first performed comparative FEA of zero Poisson's ratio metamaterials versus conventional structures to verify whether amputees wearing zero Poisson's ratio-fabricated prosthetic sockets experience reduced residual limb pressure. As shown in figure 2, ANSYS software simulated the stress and deformation of cylindrical solids (13 mm diameter) compressing both common and zero Poisson's ratio metamaterials (43.38 mm $\times$ 28.92 mm). To reflect actual conditions, the material was respectively set to Young's modulus: 1817 MPa, Poisson's ratio: 0.38, based on our measured results. The results demonstrate that the stress in the zero Poisson's ratio metamaterials decreased from 562.39–554.02 MPa, which would benefit prosthetic socket applications. More importantly, under compression conditions, the zero Poisson's ratio metamaterial exhibits significant deformation compared to traditional structures. The contact angle between the cylinder and the bottom structure increases from approximately 75°–100°, indicating a significant improvement in contact stability. The designed unit cell of the zero Poisson's ratio metamaterials is depicted in figure 2(c), the unit cell is designed to be fully symmetrical to ensure uniform mechanical behavior during compression. In the previous work [30], this metamaterial showed the lowest specific energy absorption, reflecting low compressive stiffness that enables predetermined displacement under minimal force. When integrated into the patellar tendon region, this directly reduces stress concentration and improves comfort, fulfilling the design's core objective. The geometric parameters of the unit cell are defined by a strut angle (θ) of 45° and a uniform strut length (L) of 1.56 mm. To ensure manufacturability within 3D printing resolution constraints, a wall thickness (t) of 1 mm was adopted, yielding an overall unit cell size of 7.23 mm in all three dimensions.

2.2. Construction of residual limb model

Before designing the prosthetic socket, we obtained image data of the amputee's residual limb by 256-row detector CT system (Revolution CT, GE Healthcare, USA). Given the prevalence of soft tissue deformation in amputees undergoing CT scans while in the supine position, the gel liner

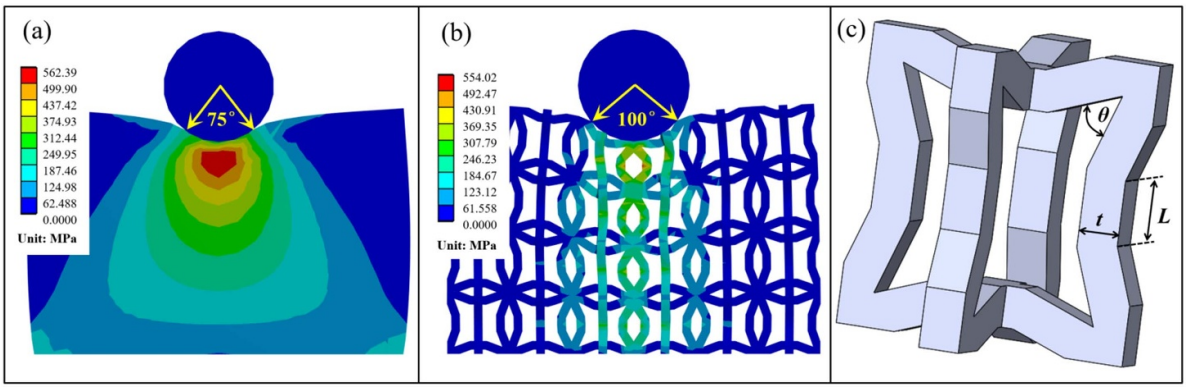

Figure 2. Comparison of stress distribution between common and zero Poisson's ratio metamaterials. (a) common structure, (b) zero Poisson's ratio metamaterials, (c) unit cell of metamaterials.

(circled section) was worn to the residual limb to minimize tissue deformation, as shown in figure 3(a). Subsequently, we acquired CT images in DICOM format with a layer thickness of 1.25 mm, and integrated images to create a comprehensive 3D model using MIMICS software. This methodology involved classifying skin, fat, and muscle as soft tissue, and non-essential components such as the meniscus, cartilage, and ligaments were omitted from the analysis. Bone and limb models were segmented based on differing grayscale values (bone: 90–1703; limb tissue: −150–1703), followed by void filling and smoothing. As shown in figure 3(b), the amputee exhibits extensive bone spurs (osteophytes), causing abnormal adhesion between the tibia and fibula. This condition is attributed to the amputee's genetic factors and prosthetic socket use habits. Besides, the bottom indentations of soft tissue were attributed to inherent scarring features, see figure 3(c). Therefore, subsequent software iterations are necessary to refine models before performing FEA.

Furthermore, the above model exhibits defects such as tiny holes and protrusions. Therefore, subsequent shape processing was performed on the models above. Initially, the bone models were separated into femur, patella, tibia, and fibula components. Subsequently, protrusions were eliminated through removing spikes operations on the respective models, and the surfaces were smoothed and repaired utilizing noise reduction, relaxation, and sandpaper sanding. This step is crucial for meshing the models in subsequent FEA. Finally, the processed bone and limb models were surface fitted to acquire solid models in STP format.

2.3. Design of prosthetic socket

Before designing the prosthetic socket model, statistical analysis of the pressure-tolerant and pressure-sensitive zones of the residual limb is essential. Traditionally, prosthetic technicians manually palpate the amputee's residual limb to assess soft tissue hardness, determining pressure-tolerant capacity and pressure sensitivity based on soft tissue thickness. Zones close to the bone are identified as pressure-sensitive and unsuitable for bearing pressure, whereas areas with thicker soft tissue are designated as pressure-tolerant. Thus, by using the amputee's musculoskeletal model and the biomechanical principles [31, 32], pressure-sensitive areas (red zone) and pressure-tolerant areas (green zone) are delineated, as shown in figure 4.

Subsequently, the design software creates the prosthetic socket based on the musculoskeletal model of the residual limb, as illustrated in the workflow in figure 5. First, a contour line is cut along the patellar base, both sides of the femur, and the posterior side of the tibia (figure 5(b)). Pressure-tolerant and pressure-sensitive zone surface groups are then generated using the musculoskeletal information of the residual limb in transparency mode (figures 5(c) and (e)), with corresponding offsets applied according with case [33, 34]. This includes a 4 mm inward offset in the patellar tendon area, 2 mm in the popliteal depression area, and 1.5 mm in the lateral and medial tibial areas. Pressure-sensitive zones feature a 2 mm outward offset at the tibial crest and small bony protrusions (figures 5(d) and (f)). Scarred areas on the residual limb are subsequently smoothed (figure 5(g)). Since the distal fibula is bony, the length of the socket at the bottom is extended by 10 mm (figure 5(h)). The residual limb model is then smoothed overall (figure 5(i)), followed by a 5 mm global offset to reserve space for the liner thickness (figure 5(j)). The liner model is thickened by 5 mm to form the socket (figure 5(k)). Finally, the top of the model is smoothed to establish the initial shape of the prosthetic socket (figure 5 (l)).

2.4. Socket with zero Poisson's ratio metamaterials

As shown in figure 6(a), we utilized 3D scanning technology to obtain the original 3D model of the prosthetic socket that is currently worn, then added the socket platform to attach the prosthetic foot. In figure 6(b), the socket platform was also added to biomechanically designed prosthetic socket. Furthermore, to reduce the pressure on the residual limb pressure-tolerant zone, we designed the zero Poisson's ratio metamaterials in the patella area of the socket (approximately

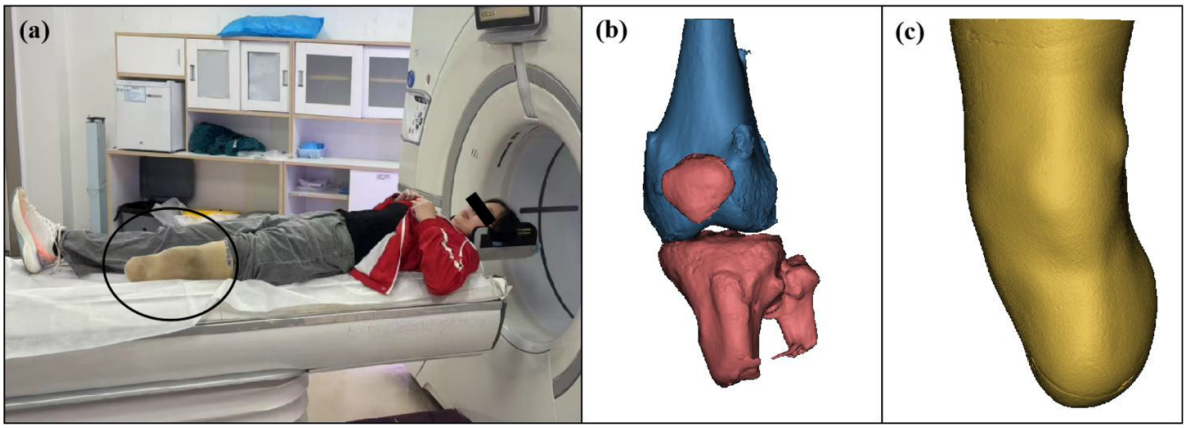

Figure 3. Construction of the residual limb model. (a) CT pictures, (b) bone model, (c) limb model.

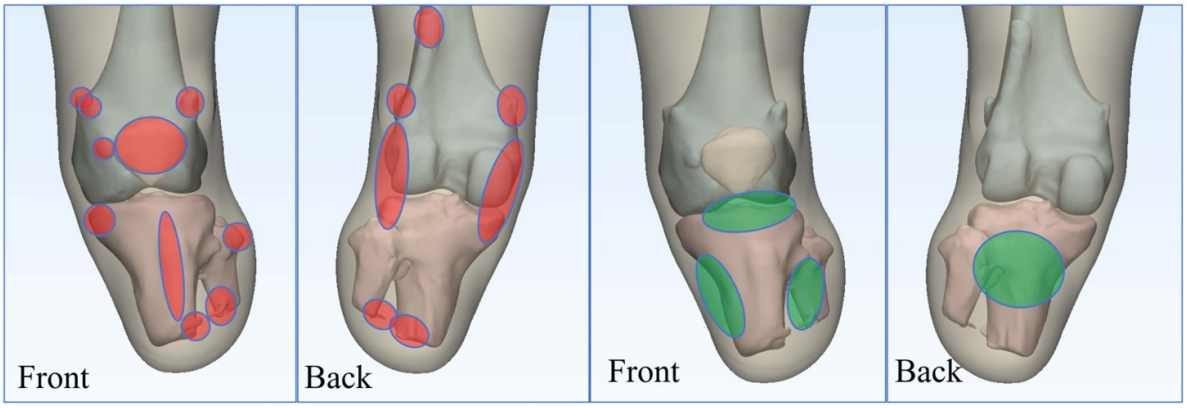

Figure 4. Pressure-sensitive (red area) and pressure-tolerant (green area) zones of the residual limb.

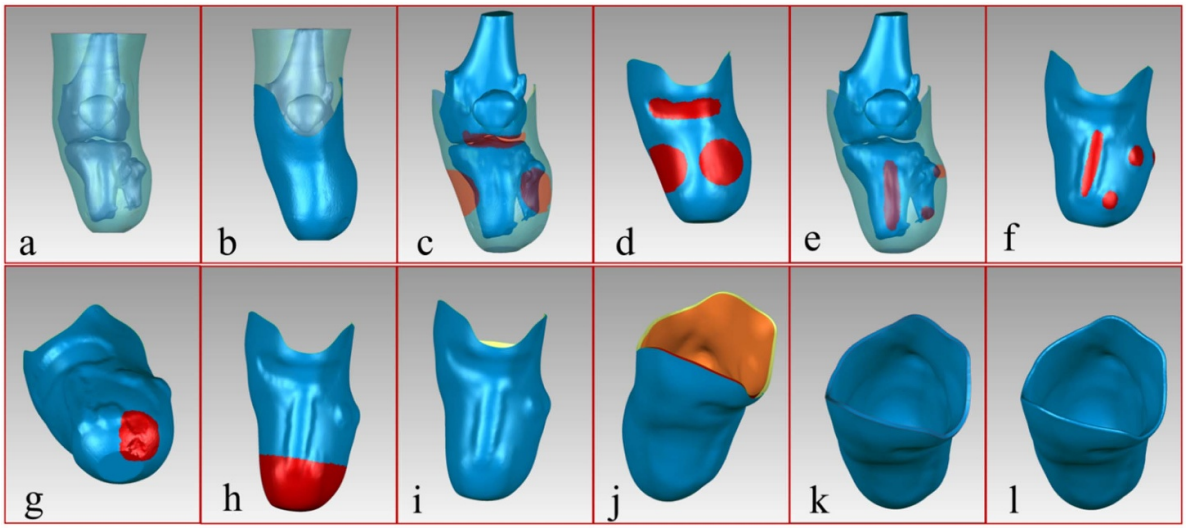

Figure 5. Design flowchart of the prosthetic socket.

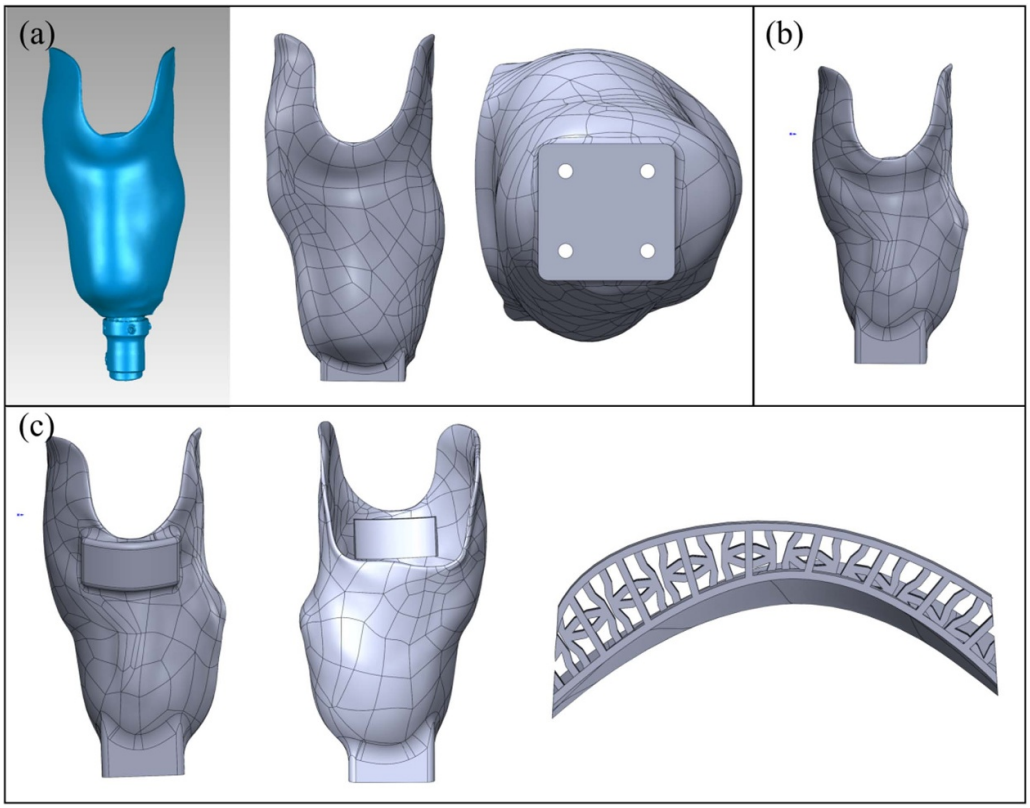

Figure 6. Prosthetic socket with metamaterials. (a) 3D scanned original prosthetic socket model, designed prosthetic socket with platform, (b) biomechanically designed socket model, (c) prosthetic socket with zero Poisson's ratio metamaterials.

60 mm in length and 30 mm in width), as shown in figure 6(c). First, we thickened the outer layer of this area in the prosthetic socket to ensure it could accommodate the zero Poisson's ratio metamaterials. Then approximately 36 (9×4) zero Poisson's ratio units are arranged, with specific unit dimensions provided in the above sections [30]. Additionally, the 1 mm prosthetic socket inner layer was designed to isolate the prosthetic liner. Finally, we conducted FEA to simulate the wearing of the original socket (figure 6(a)), biomechanically designed socket (figure 6(b)), and zero Poisson's ratio metamaterials socket (figure 6(c)) on the residual limb, enabling observation of stress distribution patterns.

2.5. FEA of prosthetic socket, liner, and residual limb

Before initiating the FEA, the systematic assembly was implemented for the prosthetic socket, liner, bone, and residual limb components. Given the inherent anatomical congruence between the prosthetic socket and residual limb models, spatial integration of the bone, soft tissue, prosthetic liner, and socket subsystems was achieved through Boolean union operations. To account for manufacturing tolerances at the socket-liner interface and eliminate potential prestress, a controlled vertical displacement was imposed on the socket model, thereby establishing a neutral-contact initial configuration for subsequent analysis.

Since zero Poisson's ratio metamaterials are sensitive to Young's modulus of the socket material, we machined the dog bone specimen from the 3D-printed socket materials and performed tensile experiments to measure its Young's modulus at 1817 MPa, as shown in figure 7(a). Additionally, the multiphysics framework incorporated four material domains: bone, soft tissue, prosthetic liner, and socket. Isotropic linear elastic constitutive models were adopted for bone (Young's modulus: 10 GPa, Poisson's ratio: 0.3), soft tissue (0.3 MPa, 0.48), prosthetic liner (2 MPa, 0.4), and socket (1817 MPa, 0.38) based on a convergence-optimized protocol [31, 32]. To balance computational efficiency and simulation accuracy, the entire model was discretized with two mesh sizes: 7 mm and 5 mm. The results demonstrated that the stress distributions for both meshes were nearly identical. The maximum stress values were 0.11531 MPa and 0.11842 MPa, respectively, with a difference of only 2.6%. Thus, the 5 mm mesh was deemed sufficiently accurate for this work.

A multi-scale meshing strategy was adopted for the finite element model of the prosthetic socket with zero Poisson's ratio metamaterial. The global mesh consisted of 5 mm tetrahedral elements to balance computational efficiency with simulation accuracy. Local refinement to 3 mm elements was applied at the critical liner-socket interface to resolve contact stresses. Furthermore, due to the metamaterial's thin 1 mm profile, the finer 0.5 mm tetrahedral mesh was implemented there to capture its mechanical response accurately. This

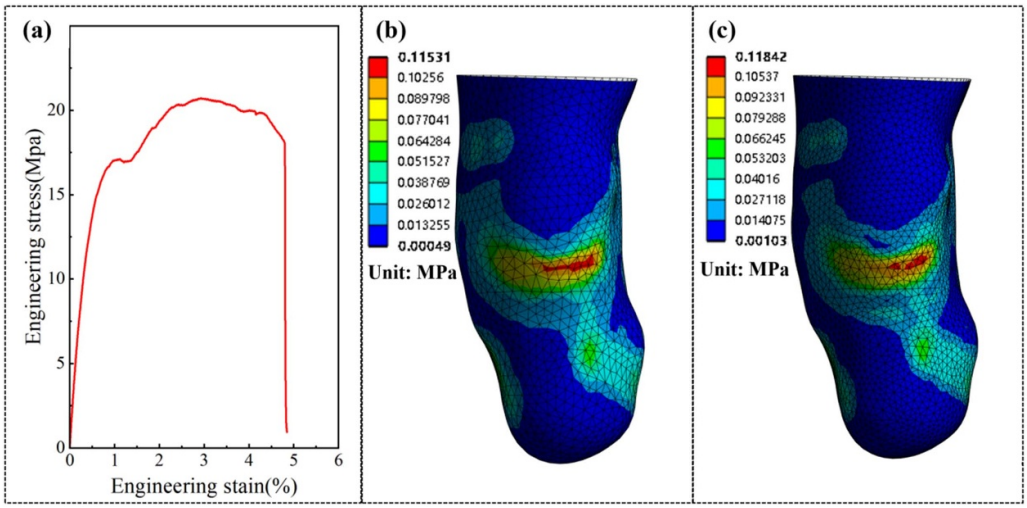

Figure 7. Skin stress distribution with the original prosthetic socket. (a) Stress–strain curve of prosthetic socket materials, (b) 7 mm mesh, (c) 5 mm mesh.

graded discretization scheme, illustrated in figure 8, ensures the precise resolution of interfacial stress gradients while maintaining computational tractability.

Surface interactions utilized a penalty-based contact algorithm ($\mu = 0.5$) to enforce non-penetration between the prosthetic liner and socket, while bone-soft tissue and soft tissue-liner interfaces were defined as fully bonded. The simulation process encompassed two clinically critical phases: prosthesis donning and static weight-bearing. During the donning phase, a 100 mm vertical displacement was applied to the femoral axis while constraining the prosthetic socket base, generating pre-stress conditions reflective of clinical fitting procedures. For standing simulation, physiological standing loads equivalent to 52 kg body mass were imposed at the femoral head interface, replicating the biomechanical loading environment of upright posture. This sequential approach captured both the initial stress state during donning and functional performance under physiological loads.

As shown in figure 9(a), when the residual limb wears the original prosthetic socket, the stress areas are primarily concentrated in the patellar tendon, popliteal depression, and minor bone spur areas, such as the left tibial bone spur. Due to the presence of bone spurs at the residual limb base, the distal tibia is designed with appropriate external offset, resulting in minimal distribution in this pressure-sensitive area. In this configuration, the maximum stress on the skin surface corresponding to the traditional socket concentrates at the patellar tendon area, specifically 0.11842 MPa. As illustrated in figure 9(b), since biomechanically designed prosthetic socket also follows the biomechanical principles of the residual limb, the skin stress distribution similarly focuses on the patellar tendon, popliteal depression, and minor bone spur areas, such as the small bone spur above the left patellar tendon. However, due to the smaller offset design in the patellar tendon area, the maximum pressure at this location reaches 0.09784 MPa. Figure 9(c) demonstrates the designed prosthetic socket with zero Poisson's ratio metamaterials. As the zero Poisson's ratio design specifically concentrates on the patellar tendon area, the skin stress in this area decreases from 0.09784 MPa to 0.083739 MPa. This reduction occurs because the zero Poisson's ratio metamaterials undergo deformation under compression, thereby alleviating stress concentration in the patellar ligament area. Additionally, the overall stress distribution pattern of the residual limb remains largely consistent, still mainly concentrated in the patellar tendon and popliteal depression areas.

3. Human testing

As shown in figure 10(a), biomechanically designed prosthetic socket and zero Poisson's ratio metamaterials were fabricated using photosensitive resin via stereolithography with a layer thickness and dimensional accuracy of 0.01 mm. Meanwhile, the prosthetic socket was assembled with steel pylon and footplate to form the prosthetic system, while the zero Poisson's ratio metamaterials were integrated. Then, flexible pressure sensors (S2054 sensor array: 160 $\times$ 80 mm^2 sensing area, 10 $\times$ 10 mm^2 persistent sensors; sampling rate: 20 000 Hz) were attached to the residual limb skin and secured with transparent tape. Finally, amputees wore their original prosthetic liners and our prosthetic system to conduct walking experiments at speed of 3 km h^{-1} for 30 s. We used the Novel Pliance-xf-32 system to measure the maximum pressure (during residual limb support phase) and took the average of the three highest pressure values as the measurement result. Figure 10(b) compares the pressure distributions at the patellar tendon for three configurations: the original prosthetic socket, biomechanically designed prosthetic socket, and the prosthetic socket with zero Poisson's ratio metamaterials.

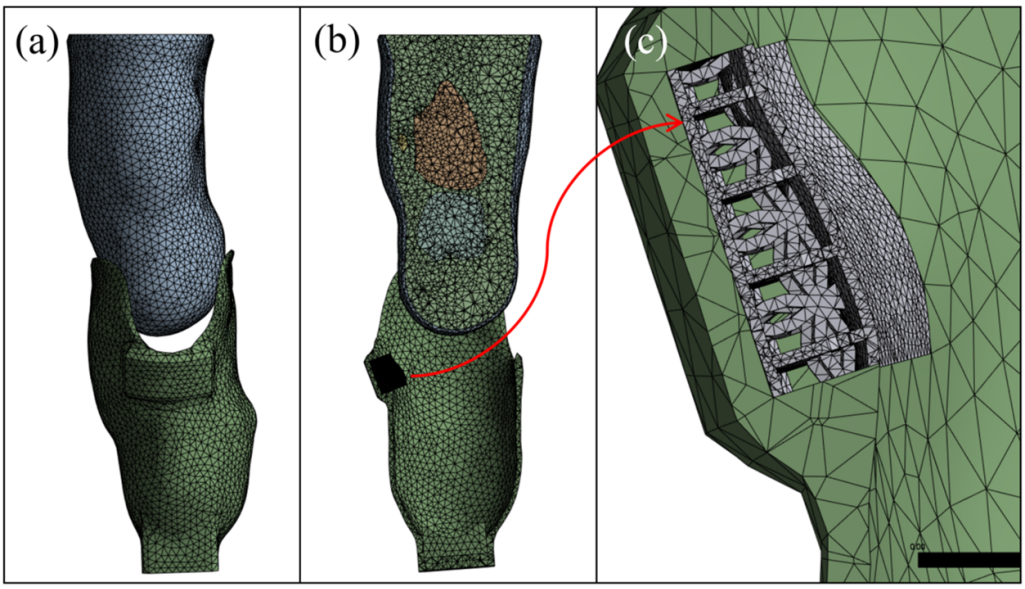

Figure 8. Typical tetrahedral mesh. (a) Surface mesh, (b) internal mesh, (c) zero Poisson's ratio metamaterials mesh.

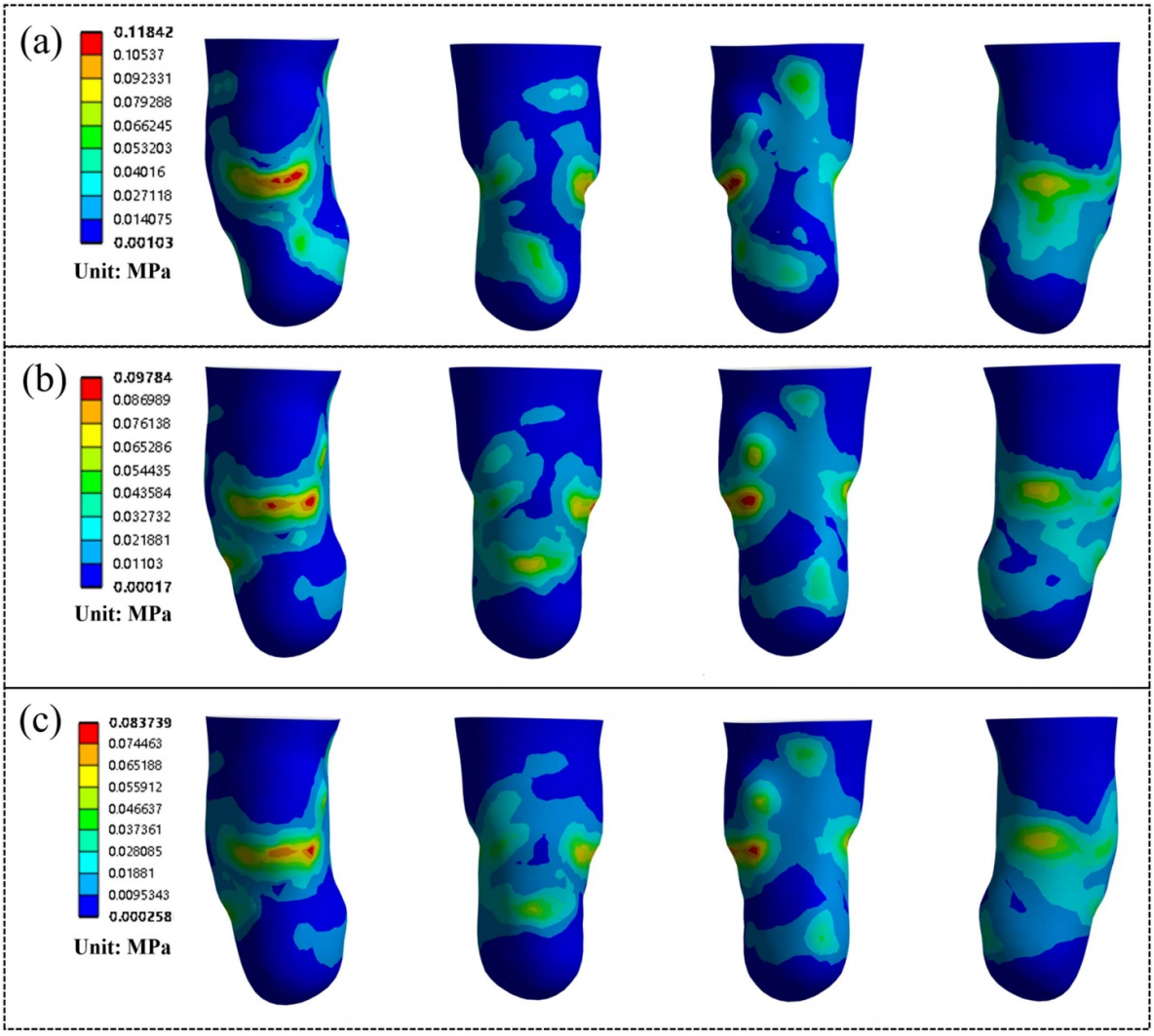

Figure 9. Skin stress distribution of the residual limb. (a) Original prosthetic socket, (b) biomechanically designed prosthetic socket, (c) designed prosthetic socket with zero Poisson's ratio metamaterials.

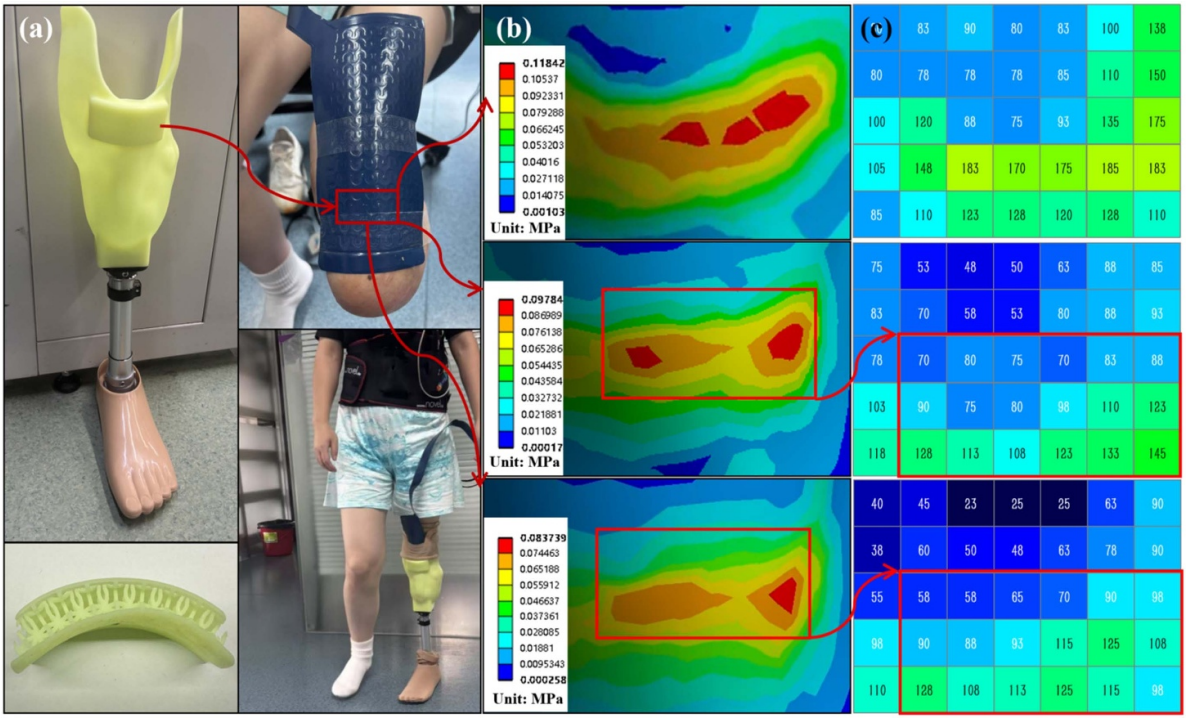

Figure 10. Residual limb pressure testing. (a) 3D printed prosthetic socket and zero Poisson's ratio metamaterials; flexible pressure sensors attached to the skin; Amputee walking for pressure measurement, (b) FEA pressure distribution, from top to bottom: original prosthetic socket, biomechanically designed prosthetic socket, designed prosthetic socket with zero Poisson's ratio metamaterials, (c) maximum pressure (Unit: kPa) distribution during walking, red box (length 60 mm, width 30 mm) indicates the area with zero Poisson's ratio metamaterial.

FEA simulations yielded maximum pressures of 118.42 kPa, 97.84 kPa, and 83.74 kPa, respectively. While discrepancies exist between simulations and experimental measurements, the overall trends align. These deviations arise from the simulation's simplified assumptions: soft tissues were modeled as a homogeneous continuum with linear material properties to enhance computational convergence, whereas real soft tissues (muscle, fat, skin, ligaments) exhibit heterogeneous biomechanical behavior. As shown in figure 10(c), the original socket generated a peak pressure of 185 kPa during walking, exceeding the residual limb's pain threshold (as reported by amputees during interviews), causing significant discomfort. Biomechanically designed socket reduced the peak pressure to 145 kPa, consistent with simulation predictions. Furthermore, the prosthetic socket with zero Poisson's ratio metamaterials achieved an additional 11.7% reduction in peak pressure (128 kPa). Notably, the total pressure within the metamaterials area (red box: 60 × 30 mm) remained nearly unchanged (1792 kPa vs. 1743 kPa), demonstrating that the zero Poisson's ratio metamaterials effectively redistribute pressure by mitigating peak stresses while maintaining overall pressure-tolerant capacity.

To compare the effects of zero Poisson's ratio metamaterial prosthetic socket on pressure distribution in amputee's residual limb, we conducted squatting experiments on amputees. Since patellar pressure is highest during squatting, this movement best demonstrates the advantages and disadvantages of this metamaterials. Additionally, a motion capture system (VICON, sampling frequency: 100 Hz) and AMTI force plates were employed to record the lower limb kinematic data of amputees wearing the original and zero Poisson's ratio metamaterial prosthetic socket, to assess its effect on amputees' gait and bilateral pressure, as shown in figure 11. Figure 11(a) compares the kinematic characteristics of knee joints and ground reaction force (GRF) during squatting motions for an amputee wearing both the original and zero Poisson's ratio metamaterials prosthetic socket. When using the original socket (see figure 11(b)), the peak knee flexion angle of the intact limb reached 83.4°, while the residual limb exhibited compensatory kinematics with a maximum knee angle of 90.7° at 4.2 s. In contrast, wearing the socket with zero Poisson's ratio matematerials significantly improved bilateral symmetry: the Pearson correlation coefficient between intact and residual limb knee angles increased from 0.992 to 0.999, and peak flexion angles improved to 104.1° (intact) and 102.3° (residual), approaching the physiological range of 100° to 110°, thereby enabling more natural movement patterns, as shown in figure 11(c).

GRF also demonstrated notable improvements. Both sockets maintained a symmetrical baseline GRF of 260 N (equivalent to 52 kg body weight). However, during squat ascent, the original socket exhibited asymmetric force peaks of 350 N (intact) and 190 N (residual), with their sum exceeding 520 N due to inertial effects during standing transitions. The

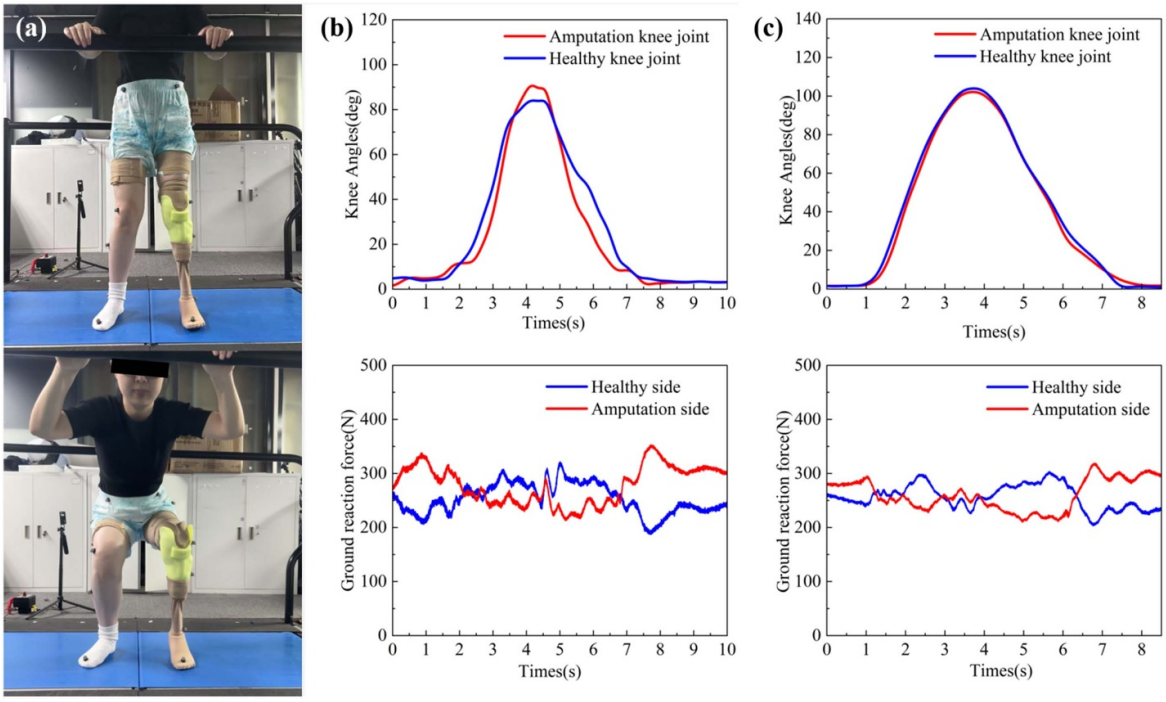

Figure 11. Human testing on a unilateral below-knee amputee. (a) Standing and squatting testing, knee joint angles and GRF wearing (b) the original prosthetic socket and (c) the zero Poisson's ratio metamaterials prosthetic socket, respectively.

prosthetic socket with zero Poisson's ratio metamaterials reduced this asymmetry to 316 N (intact) and 204 N (residual). Notably, during deep squat phases (knee flexion $>85°$), the socket with zero Poisson's ratio metamaterials generated consistent GRF magnitudes ($\sim$360 N between 2.8–4 s), whereas the original socket failed to maintain force continuity, further validating the enhanced biomechanical performance of our designed prosthetic socket.

4. Discussion & future work

We have preliminarily validated our design through standing and squatting tests on unilateral below-knee amputees. Compared with the prosthetic socket (185 kPa) daily used by amputee, biomechanically designed prosthetic socket exerts 145 kPa pressure. Furthermore, the application of zero Poisson's ratio metamaterials (128 kPa) reduces peak pressure by additionally 11.7%. Current research on prosthetic socket designs primarily address extending service life (adjustable socket), enhancing comfort in pressure-sensitive zones of the residual limb (hybrid soft-rigid material socket), and bacterial growth caused by skin overheating (Perforated heat dissipation or additional fans sockets). In contrast to these approaches, this study pioneers the novel application of zero Poisson's ratio metamaterials in prosthetic sockets, successfully reducing peak pressure in pressure-tolerance areas. This advancement significantly enhances comfort during daily movements, such as walking and particularly stair climbing (where residual limbs endure higher peak pressures). Additionally, these metamaterials offer universal adaptability for sockets of any residual limb shape and can be easily fabricated via 3D printing. While the current design has only undergone short-term verification, its long-term durability requires further investigation.

It is noteworthy that during walking, the socket endures complex dynamic loading conditions beyond vertical compression, including upward pulling forces during leg lifting and significant impact forces at heel strike. Thus, we will focus on characterizing dynamic stress and shear force distribution patterns during ambulation to enhance socket functionality under realistic gait conditions. Furthermore, the Young's modulus of current 3D-printed photosensitive resin materials remains lower than traditional socket materials, while their fatigue resistance requires thorough evaluation. Concurrently, we will investigate the fatigue resistance of various materials (such as nylon, polylactic acid, and acrylonitrile butadiene styrene) [35] and structural sockets prepared using 3D printing technology under realistic service conditions. Additionally, systematic optimization of the structural geometry, dimensional parameters, layer thickness, and material properties of zero Poisson's ratio metamaterial units will further broaden their application potential [36]. Ultimately, we will address the mechanical challenges of dynamic loading and the material limitations of 3D printing in prosthetic socket applications in the future.

5. Conclusion

This work describes a novel prosthetic socket with zero Poisson's ratio metamaterials in pressure-tolerance zone. Through CT modeling, FEA, flexible pressure measurements, and motion capture system testing, our designed

prosthetic socket significantly reduced peak pressures and improved bilateral symmetry. Specifically, the socket model was designed based on musculoskeletal model constructed from CT data, and zero Poisson's ratio metamaterials were introduced into the socket patellar tendon area. FEA results showed that biomechanically designed socket reduced the peak pressure by 17.4% compared to the original socket, which was further reduced to 29.3% with the zero Poisson's ratio metamaterials socket. Flexible pressure sensor measurements during gait showed a reduction in peak pressure from 185 kPa (original socket) to 145 kPa (biomechanically designed socket) and 128 kPa (zero Poisson's ratio metamaterials socket). The reduction ratios were 21.6% and 30.8%, respectively, which was consistent with the FEA predictions. Squat tests demonstrated that the difference in knee angle between the residual limb and the intact limb was reduced from 7.3° to 1.8° after wearing the zero Poisson's ratio metamaterials socket. GRF analysis showed that asymmetric loading on the residual limb was reduced from 160 N to 112 N. These observations suggest that the zero Poisson's ratio metamaterials socket is effective in reducing peak pressure, thereby improving amputee's comfort and quality of life.

Data availability statement

All data that support the findings of this study are included within the article (and any supplementary files).

Acknowledgment

This work was supported by the National Natural Science Foundation of China (No. 52405299), in part by the Key R&D Project of Hainan Province (Grant Nos. ZDYF2022SHFZ302, ZDYF2022SHFZ275), in part by the Shenzhen basic research key project (Project No. JCYJ20220818101407016), in part by the Shenzhen-Hong Kong-Macao Science and Technology Project (Category C) (Project No. SGDX20220530111005036), and in part by the National Natural Science Fund for Excellent Young Scientists Fund Program (Overseas).

Author contributions

Sheng Li 0000-0002-0093-6509
Writing – original draft (lead)

Mahdi Bodaghi 0000-0002-0707-944X
Supervision (supporting), Writing – review & editing (supporting)

Guoxin Fang 0000-0001-8741-3227
Supervision (supporting)

Wenbin Qiu
Writing – review & editing (supporting)

Xinyu Wu
Resources (supporting)

References

[1] McDonald C L, Westcott-mccoy S, Weaver M R, Haagsma J and Kartin D 2021 *Prosthet. Orthot. Int.* **45** 105–14
[2] Hong W, Kumar N A, Patrick S, Um H-J, Kim H-S, Kim H-S and Hur P 2022 *IEEE Robot. Autom. Lett.* **7** 11228–35
[3] Barontini F, Catalano M G, Grioli G, Bianchi M and Bicchi A 2021 *IEEE Robot. Autom. Lett.* **6** 1785–92
[4] Gao F, Liu Y and Liao W-H 2019 IEEE/ASME Trans. Mechatronics **24** 1775–84
[5] Li S, Xie B, Chen Y, Wu X, Fang G, Zhang Y and Gao F 2024 *2024 IEEE Int. Conf. on Cyborg and Bionic Systems (CBS)* pp 27–32
[6] Nayak C, Singh A, Chaudhary H and Tripathi A 2016 *Biomed. Eng. Appl. Basis Commun.* **28** 3
[7] Gao F, Liu Y and Liao W-H 2018 *J. Mech. Des.* **140** 075003
[8] Weathersby E J, Garbini J L, Larsen B G, McLean J B, Vamos A C and Sanders J E 2021 *IEEE Trans. Biomed. Eng.* **68** 36–46
[9] Baldock M, Pickard N, Prince M, Kirkwood S, Chadwell A, Howard D, Dickinson A, Kenney L, Gill N and Curtin S 2023 *J. Neuroeng. Rehabil.* **20** 147
[10] Norli M H M, Sukimi A K A, Ramlee M H, Mahmud J and Abdullah A H 2024 *Int. J. Technol.* **15** 455
[11] Paterno L, Ibrahimi M, Gruppioni E, Menciassi A and Ricotti L 2018 *IEEE Trans. Biomed. Eng.* **65** 1996–2010
[12] Greenwald R M, Dean R C and Board W J 2003 *J. Prosthet. Orthot.* **15** 107–112
[13] Carrigan W, Nothnagle C, Savant P, Gao F and Wijesundara M B J, 2016 *2016 6th IEEE Int. Conf. on Biomedical Robotics and Biomechatronics (Biorob)* pp 574–9
[14] Sengeh D M and Herr H 2013 *J. Prosthet. Orthot.* **25** 129–37
[15] Comotti C, Regazzoni D, Rizzi C and Vitali A, 2015 *Proc. of the 3rd 2015 Workshop on ICTs for Improving Patients Rehabilitation Research Techniques* pp 42–45
[16] Webber C M and Davis B L 2015 *J. biomech.* **48** 1294–9
[17] Han Y, Liu F, Dowd G and Zhe J 2015 *Appl. Therm. Eng.* **82** 246–52
[18] Shirzad M, Zolfagharian A, Bodaghi M and Nam S Y 2023 *Eur. J. Mech. A* **98** 104905
[19] Hamzehei R, Bodaghi M, Iglesias Martinez J A, Ji Q, Ulliac G, Kadic M, Wang C, Zolfagharian A and Wu N 2023 *Adv. Eng. Mater.* **25** 2201842
[20] Bodaghi M, Damanpack A R, Hu G F and Liao W H 2017 *Mater. Des.* **131** 81–91
[21] Bodaghi M and Liao W H 2019 *Smart Mater. Struct.* **28** 045019
[22] Wallbanks M, Khan M F, Bodaghi M, Triantaphyllou A and Serjouei A 2021 *Smart Mater. Struct.* **31** 023002
[23] Dara A, Johnney Mertens A and Raju Bahubalendruni M 2023 *Proc. Inst. Mech. Eng. L* **237** 906–13
[24] Dara A, Bahubalendruni M V A R, Johnney Mertens A and Balamurali G 2022 *Mater. Today Commun.* **31** 103286
[25] Ashok D, Raju Bahubalendruni M V A, Mertens A J and Balamurali G 2022 *Proc. Inst. Mech. Eng. E* **236** 2434–40
[26] Ashok D, Bahubalendruni M V A R, Mhaskar A, Choudhary V, Balamurali G and Turaka S 2023 *Proc. Inst. Mech. Eng. E* **239** 2419–29

[27] Bejjani R, Odelros S, Öhman S and Collin M 2021 *Proc. Inst. Mech. Eng.* **235** 114–28
[28] Mansoori H, Hamzehei R and Dariushi S 2022 *Proc. Inst. Mech. Eng. L* **236** 647–62
[29] Hamzehei R, Zolfagharian A, Dariushi S and Bodaghi M 2022 *Smart Mater. Struct.* **31** 3
[30] Hamzehei R, Serjouei A, Wu N, Zolfagharian A and Bodaghi M 2022 *Adv. Eng. Mater.* **24** 2200656
[31] Zhang M and Roberts C 2000 *Med. Eng. Phys.* **22** 607–12
[32] Lee D R C *et al* 2024 *Sci. Rep.* **14** 25833
[33] Nehme G and Ghalambor S 2014 *J. Prosthet. Orthot.* **26** 194–204
[34] Faustini M C, Neptune R R, Crawford R H, Rogers W E and Bosker G 2006 *IEEE Trans. Neural Syst. Rehabil. Eng.* **14** 304–10
[35] Dara A, Mertens J, Gunji B and Bahubalendruni M V A R 2025 *Mater. Today Commun.* **44** 111953
[36] Chandra C R, Ashok D, Anil P, Kasireddy S R and Bahubalendruni M V A R 2025 *Int. J. Prot. Struct.* 1–20